

Enhancing the injectability of high concentration drug formulations using core annular flows

Vishnu Jayaprakash, Maxime Costalonga, Somayajulu Dhulipala and Kripa K. Varanasi*

V.J. Author 1, Dr. M.C Author 2, S.D Author 3, Prof. K.K.V Author 4

Department of Mechanical Engineering, Massachusetts Institute of Technology,

77 Massachusetts Ave, Cambridge, MA, 02139

E-mail: kripa@mit.edu

Keywords: Drug delivery, Microfluidics, Personalized medicine

Abstract

Highly concentrated biologic drug formulations would offer tremendous benefits to global health, yet they cannot be manually injected using commercial syringes and needles due to their high viscosities. Current approaches to address this problem face several challenges such as cross-contamination, high cost, needle clogging and protein inactivation. This work reports a simple method to enhance formulation injectability using a core annular flow, where the transport of highly viscous fluids through a needle is enabled by co-axial lubrication by a less viscous fluid. A phase diagram to ensure optimally lubricated flow while minimizing the volume fraction of lubricant injected is established. The technique presented here allows for up to a 7x reduction in injection force for the highest viscosity ratio tested. The role of buoyancy-driven eccentricity in governing

This is the author manuscript accepted for publication and has undergone full peer review but has not been through the copyediting, typesetting, pagination and proofreading process, which may lead to differences between this version and the [Version of Record](#). Please cite this article as [doi: 10.1002/adhm.202001022](https://doi.org/10.1002/adhm.202001022).

This article is protected by copyright. All rights reserved.

nominal pressure reduction is also examined. Finally, the findings are implemented into the development of a double barreled syringe that significantly expands the range of injectable concentrations of several biologic formulations.

MAIN TEXT

Introduction

In 2012, worldwide biopharmaceutical sales were estimated to reach US\$163 billion, accounting for over 70% of the revenue from the top ten selling pharmaceutical products.^[1,2] Monoclonal antibodies, enzymes, peptides and recombinant therapeutic proteins are all examples of biologic drugs that have transformed the pharmaceutical industry due to their high degree of specificity, potency, and efficacy compared to conventional small-molecule drugs.^[3,4] Due to these benefits, over a thousand biologics targeting cancer, asthma, psoriasis, arthritic disease, and a wide range of infectious and non-infectious diseases are being developed.^[5–7]

Currently, these drugs are predominantly administered in low concentrations (<30mg/ml) via intravenous injections at doses ranging from 5 to 700 milligrams.^[8] Over the past few years, however, subcutaneous injection has emerged as an alternative delivery route as it (i) enables self-administration, (ii) reduces hospitalization and treatment costs, and (iii) increases patient compliance.^[8] Unlike intravenous injections, subcutaneous injections require formulations that are far more concentrated (>100mg/ml) as injection volumes are limited to 1-1.5ml per dose. This constraint arises from high back pressures that can develop in subcutaneous tissue at larger volumes.^[8,9] A non-linear relationship between formulation

concentration and viscosity makes subcutaneous formulations very viscous (20-60 cP) and therefore harder to inject, as illustrated in figure 1a: a highly viscous fluid (dyed blue) spreads significantly less than a low viscosity fluid (dyed green), when injected in a sponge at the maximal force we could apply manually (around 50N).^[10–13] Consequently, the applicable force sets a limit to the concentrations of current formulations, as shown in figure 1b. This figure reports the injection force (for a flow rate of 4ml/min through a 27G needle) as a function of concentration for four monoclonal antibody solutions of the IgG1 isotype that have been reported in literature.^[10–13] This figure also highlights the fact that an extensive range of formulation concentrations require more than 50N to be injected – the average maximum force that can be applied in a pinching motion to a syringe for subcutaneous injections.^[14–16]

While larger needle gauges or prolonged injection times through the use of syringe pumps could overcome challenges associated with the low injectability of high concentration formulations, these approaches would negate the benefits offered by subcutaneous delivery due to a larger degree of pain and the requirement of a hospital setting, respectively.^[17] Needle-free jet injectors have also been proposed as a potential pathway to enable the delivery of high viscosity formulations. However, splashback of the jet stream and blood from the injection site, combined with observations of fluids being sucked back into the injector, have been reported to contaminate the injector and subsequent doses during repeated use.^[18–21] These issues, together with the high cost of such injectors, prohibit their use in the context of self-administration, especially in the developing world.

Another recent approach consists of using particle encapsulation to create microscale carriers that can deliver highly viscous biologics.^[22] However, protein inactivation, density-based separation, needle clogging, and a higher degree of manufacturing complexity are critical problems that need to be addressed to make this approach viable.^[18,23–25] The lack of a practical methodology to inject high viscosity formulations has not only limited the applicability of subcutaneous biologic formulations but also hinders the development of new formulations, forcing developers to design formulations with lower viscosities. Therefore, there remains a pressing need to achieve injectability through a simple and inexpensive technique with minimal additions to the pharmaceutical manufacturing process, and without risk of cross-contamination.

Here we propose such a technique to enhance the injectability of highly concentrated drug formulations using core annular flows. In such a flow, a low viscosity fluid coaxially lubricates the transport of immiscible viscous fluids through the needle (figure 1c). This not only reduces the hydrodynamic resistance in the needle but also reduces shear forces on the payload material (inner fluid). Core annular flows have been explored as a lubrication technique, to facilitate the transport of viscous oils through pipelines.^[26–28] However, these flows are not widely used in practice for oil transport due the difficulty in maintaining stable, co-axial lubrication over large length scales.^[29] In microfluidics, dripping to jetting transitions of co-flowing liquids are used in droplet generators and emulsifiers.^[30–32] However, the diameter of medical needles ($\approx 200\ \mu\text{m}$) is neither in the macroscopic scale of oil pipelines nor in the microfluidic scale. Hence it is important to understand how to establish and sustain a core annular flow in such needles.

In the case of a concentric core annular flow, the Navier-Stokes equations combined with the lubrication approximation can be used to predict the attainable pressure reduction coefficient η , as a

function of the viscosity ratio $\lambda = \mu_i/\mu_o$. While these formulations can exhibit non-Newtonian behavior (specifically shear thinning) at high shear rates, only Newtonian behavior is considered in this work.^[16,33,34] This is because the shear-thinning of these formulations is not sufficient to make them injectable.^[34] The subscript i denotes quantities related to the inner (viscous) fluid, and the subscript o denotes those related to the outer (lubricating) fluid. With no-slip boundary conditions at the wall of the needle, shear and velocity continuity at the interface of the two fluids, the pressure reduction factor can be expressed as (see SI for derivation):

$$\eta = \frac{\Delta P_{\text{control}}}{\Delta P_{\text{Core annular flow}}} = \frac{r_i^4}{r_o^4} \left(2\lambda \left(\frac{r_o^2}{r_i^2} - 1 \right) + 1 \right); \quad (1)$$

Plotting this pressure reduction coefficient as a function of the flow rate ratios (figure 1d) reveals that a maximum is reached when $Q_o/Q_i \approx 0.4$, followed by a slight decrease at high flow rate ratios. Pressure reductions up to 50x can be reached in theory, in the case of $\lambda = 100$, making core annular flows a promising candidate to reduce the force needed to inject viscous formulations manually significantly. The goal of our paper is to develop a device that uses core annular flows to enable the injection of highly viscous formulations and to compare its performance to the expected pressure reduction from such flows. To achieve this, we first report the flow regimes observable in such a device and establish a regime map to indicate the flow rates and viscosity ratios at which core annular flow can be sustained in a needle. We then quantify the corresponding pressure reduction and compare our measurements with theoretical predictions. Finally, we design, fabricate, and test a co-axial, double barreled syringe to exhibit the capability of this technique to inject high concentration drug formulations.

Results

The setup shown in figure 2a was used to study the dynamics of core annular flows through a needle. Two syringe pumps were used to drive the inner viscous fluid and the outer lubricating fluid through a fluidic cross to establish the core annular flow. A digital pressure sensor (see methods) at the cross measured the pressure drop through the needle. A transparent needle was used to visualize the flow, and the dimensions of all components were chosen so that their hydrodynamic resistances are negligible compared to that of the needle (as shown in the supplementary information).^[35]

Due to the volume and dosing constraints of subcutaneous biologic injections mentioned earlier, volume fractions (of viscous payload) lower than 55% were not considered as it is undesirable to inject the same amount or more of the lubricant, than the drug formulation. In addition, figure 1d shows that the benefit of core annular flows is reduced at low viscous payload volume fractions ($Q_o/Q_i > 0.8$). Therefore, the flow rate of the inner viscous fluid was fixed at 1 ml/min, and the flow rate of the outer lubricant was varied from 0.1 to 0.8 ml/min. These values were chosen as they are in the range of flow rates required for a practical injection.^[36] Figure 2b shows a map of the observed flow regimes for different flow rate and viscosity ratios. Two regimes occur in our phase space: a viscous displacement regime at low lubricant flow rates, and a core annular flow regime as the lubricant flow rate increases. In the viscous displacement regime, the viscous fluid first fills the entire cross-section of the needle, inducing both fluids to back-flow into the lubricant inlet. However, this back-flow cannot be sustained due to the constant mass flux imposed on the lubricant, resulting in a sudden overflow of the lubricant into the needle. This flow decreases until being completely hindered once again, and the process repeats. This cyclic behavior is shown in the

temporal diagram of a cross-section of the needle (Figure 2c): it leads to unsteady and significantly worse lubrication compared to the core annular flow regime (Figure 2d).

Figure 3a reports the experimental pressure reduction coefficient (mean \pm std. error) as a function of the ratio between the lubricant flow rate and the viscous fluid flow rate, for several viscosity ratios. Experiments corresponding to the viscous displacement regime ($Q_o/Q_i \leq 0.2$) exhibit larger errors due to the cyclic nature of this state. Thus, the average pressure reduction factors in this regime are also much lower than in the case of the core annular flow regime ($Q_o/Q_i > 0.2$).

While the pressure reduction performance follows a similar trend as expected from concentric core annular flow theory, we observe a significant difference in the magnitude of the pressure reduction coefficients (predicted value for $\lambda = 20$ is $\eta \sim 10$ in concentric core annular flow while the experimental value for $\lambda = 19.5$ is $\eta \sim 4.5$). This lower performance originates from the eccentricity caused by the density difference between the two phases, as revealed in figure 3b (false-colored digital photograph of a side view of the needle demonstrating eccentricity due to buoyancy).

In order to account for the eccentricity, we solve the Navier-Stokes equations in a bipolar coordinate system, following the approach of Bentwich et al.^[37,38] By doing so, we derive a modified expression for the pressure reduction coefficient (equations S18 – S21), featuring an eccentricity parameter E , which ranges from 0 (non-eccentric) to 1 (fully eccentric) (Figure 3b). Figure 3c shows excellent agreement between the experimental measurements for the pressure reduction coefficient and those derived from the eccentric core annular flow model using $E=0.98$, indicating that the model effectively captures the performance of core annular flows in realistic conditions (i.e., without density matching). The experimental

results and the model reported here correspond to the base-line scenario where the syringe is kept horizontal. The pressure reduction achieved in the horizontal case represents the most conservative measure of the benefit offered by core annular flows. While a syringe placed perfectly vertical would not experience buoyancy induced eccentricity in the needle, any deviation from the vertical orientation rapidly leads to eccentricity. By considering the timescales of convection and eccentricity formation, we developed a model that can capture the influence of the syringe orientation and it is discussed in the supplementary information.

We demonstrated that the discrepancy between measurements and theoretical predictions of the pressure reduction coefficient is due to the buoyancy induced eccentricity of the core annular flow. Even so, our experiments show that up to a 7x reduction in pressure (for $\lambda \approx 32.9$) remains achievable, indicating that the regime of injectable concentrations can be expanded significantly using core annular flows. Therefore, to implement this knowledge into a practical device, we designed and fabricated the double barreled syringe shown in figure 4a and figure 4b. It consists of an outer barrel that contains the lubricant and an inner barrel that holds the viscous payload. A six-milliliter syringe barrel from VitaNeedle® was used as the outer barrel. The fluids are driven by corresponding outer and inner plungers with a movable outer gasket that ensures leak-proof operation. The dimensions of the barrels were chosen so that during the displacement of the plungers, the ratio of lubricant flow rate to viscous fluid flow rate is approximately 0.59, which is significantly above the threshold value of 0.2 required to sustain a core annular flow. The simplicity of this design makes it easy to manufacture, as it can be made using injection molding or blow-fill

seal processes, ensuring similar ease-of-use and cost as current commercial medical syringes and needles. Supplementary Figure 3a shows the core annular flow established in a needle connected to our double barrel syringe, indicating that it indeed operates in the core annular flow regime.

Visual evidence of the enhancement in manual injectability is shown in figure 4c, where we observe better liquid spreading in a sponge when a highly viscous fluid is injected using our double barreled syringe (dark blue) compared to a commercial syringe (light blue). In order to quantify this improvement, we compared the forces needed to inject a water-glycerin solution (26.3 cP) with our double-barreled syringe and a commercial syringe for the same volume flow rate. The injection force was quantified with a load cell (see Methods) mounted on a syringe pump (supplementary Figure 3b). The measured forces were used to calculate the force reduction coefficients, η_{DBS} and η_{needle} which are defined as shown in equation 2 and equation 3.

$$\eta_{DBS} = \frac{F_{\text{commercial syringe}}}{F_{\text{Double barreled syringe}}} \quad (2)$$

$$\eta_{needle} = \frac{F_{\text{commercial syringe}} - F_{\text{commercial syringe-without needle}}}{F_{\text{Double barreled syringe}} - F_{\text{Double barreled syringe-without needle}}} \quad (3)$$

Figure 4d shows the experimental force reduction coefficients obtained from our double barreled syringe. Both the commercial and double barreled syringe were run with and without the needle in order to quantify the resistance of the barrels. One has to mention that our proof-of-concept design suffers from significant friction between the barrels and the plungers, resulting in a low value for η_{DBS} . However, this friction can be largely eliminated by using existing syringe manufacturing techniques (such as injection molding to make more appropriately sized gaskets). Plunger break-loose

and glide forces have largely been minimized using these techniques in conventional syringes as they lie in the range of 1-9N compared to the 50N manual injectability threshold.^[39] The larger variability observed for the needle (η_{DBS}) is due to the error propagation operations carried out to isolate the resistance of the needle alone. when the contributions of the barrels are removed, we observe a force reduction coefficient of 5 in the needle. This value lies within the theoretical prediction of the eccentric model with the eccentricity parameter $E = 0.98$, therefore emphasizing that the partially eccentric model accurately captures the performance of the proof-of-concept double barreled syringe.

Discussion

The significant force reduction coefficient achieved here demonstrates the promise of the core annular flows to increase the threshold concentrations of biologic drugs that can be manually injected. Figure 4e indeed shows the increases in concentrations that are possible for eleven monoclonal antibody solutions reported in literature, while keeping injection force at a nominal 25N. It reveals that we can double (formulation 6) and even triple (formulation 3) the injectable concentration for specific monoclonal antibody formulations using the double barreled syringe.^[10–13] Furthermore, the reduction of force for lower concentration formulations could enable faster injections, or the use of smaller needles, resulting in less pain for patients.^[17]

A key feature to keep in mind in the design of the double barreled syringe is wettability. Indeed, if the inner fluid preferentially wets the interior needle surface, the outer lubricant flow might fail to coaxially lubricate the inner fluid, leading to an unstable core annular flow and, therefore, tremendous loss in the benefits of core annular flow.^[32,40,41] This wetting criteria is why HFE-7500

was chosen as the model lubricant for this study, as HFE 7500 is more wetting towards the needle than the viscous aqueous payload. This is shown in supplementary figure 4, where HFE 7500 is observed to be thoroughly wetting on PTFE in the presence of glycerol (the viscous, model payload). This favorable wetting may be the reason why the flow is not wholly eccentric in our experiments ($E = 0.98$).

Our proposal to use immiscible and biocompatible lubricants is motivated by a wealth of literature on immiscible vaccine and drug adjuvants. For example, squalene and other oil-based adjuvants have been used in thousands of patients at concentrations between (5-52%) (volume of immiscible oil/volume of aqueous components) in several types of injections, including subcutaneous injections without affecting drug formulation efficacy.^[42–44] Here we used HFE-7500 as a model lubricant to demonstrate the pressure reduction benefits of core annular flows, but we understand that each drug formulation will have to be tested on our platform to identify the most appropriate lubricant-drug combination. The framework established here could also be used to explore aqueous and miscible lubricants. Supplementary figure 5 shows an example of water used as a lubricant and a mixture of glycerol and water used as the viscous inner fluid. While such miscible lubricants could allow for even safer injections into patients, buoyancy based eccentricity could lead to stratified flows rather than co-axial lubrication due to a lack of preferential wetting of the lubricant on the needle surface. A lower pressure reduction coefficient of $\eta \approx 2.6$ was measured for $Q_o/Q_i = 0.7$ and $\lambda \approx 26$ when water was used as a lubricant compared to $\eta \approx 6$ for the identical conditions with the preferentially-wetting HFE-7500. However, the design of the double barrel syringe can be optimized for water lubrication by balancing the different time scales (convection, eccentricity formation and mixing – defined in the supplementary information) to mitigate eccentricity and promote coaxial

lubrication as discussed in the supplementary information. Such designs will be explored in future studies.

The benefits observed in the core annular flow-based injection technique could be expanded to other subcutaneous delivery methods as well. Micro-needle patches, for example, could be made with smaller needles or could be used for shorter periods of time if the resistance to flow is reduced using core annular flows. This methodology also holds substantial promise for applications beyond biopharmaceuticals. For example, the lubricating effect of core annular flows could be used to inject other high viscosity or non-Newtonian fluids, such as bone putty or hydrogels. The reduced shear in such flows could also be applied to handle and dispense sensitive or primary cells where low shear is essential to prevent damage. ^[45–48]

In conclusion, we have demonstrated a simple, yet efficient technique to enhance the injectability of high concentration biopharmaceuticals using core annular flows. We established a regime map of flow rates and viscosity ratios required to attain stable core annular flow while minimizing the flow rate of the lubricant. We found that significant pressure reduction can be achieved in core annular flows for a variety of payload viscosities. We achieved practically up to a 7x reduction in pressure for a viscosity ratio of 33. In addition, we examined the role of buoyancy-induced eccentricity and compared our measurements to predicted pressure reduction in such eccentric core annular flows. We found that this model accurately captures the results of our experiments. Finally, we applied this knowledge to design, fabricate and test a prototype double barreled syringe. We showed substantial pressure reduction (up to 5x reduction for $\lambda = 26$) in our syringe which is consistent with our eccentric flow model, therefore significantly expanding the regime of injectable viscosities for biologics without increasing costs, risk of cross-contamination or manufacturing complexity.

Materials and Methods

Fluid preparation and characterization

Fluid preparation

Mixtures of glycerol and water of different viscosities were used as the inner fluid in all experiments.

HFE-7500 + 2wt% fluorosurfactant (obtained from RAN Biotechnologies) was used as the lubricant.

Rheology

A TI ARG-2 rheometer was used to measure the viscosity of all the samples. A 40mm 2° cone geometry was used to measure the viscosity of all the glycerol solutions. Stepped flow tests were done where the shear rate was varied from 10s^{-1} to 500s^{-1} . A 60mm plate geometry was used to measure the viscosity of HFE 7500. Here, the shear rate was varied from 1s^{-1} to 100s^{-1} .

Contact angles

Contact angle measurements were done using a Ramé'-Hart contact angle goniometer.

Experimental setups

Pressure reduction measurements

Harvard apparatus PHD ULTRA™ syringe pumps were used to drive the fluids. A fluidic cross with 1/8" NPT female fittings was used to establish the core annular flow. Specifically, the high viscosity fluid flowed through a (1/16" OD, 0.0575" ID) tube that traveled through the entire cross and a Luer adapter before entering the hub of the needle. The lubricant was brought through one of the branches in the cross and was allowed to exit to the needle coaxially with the inner viscous fluid. A 304.8 μm ID, 2" long PTFE needle was used in all experiments. The final branch of the cross housed a

Honeywell[®] 26PC series pressure sensor. The sensor is connected to a DC power supply and its output is measured using a Keithley[®] 2450 sourcemeter operated as a voltmeter.

Testing the double barreled syringe

An Omega engineering LC 307 series load cell was used to measure the force on the plunger. The load cell was attached to the driving plate of the syringe pump and a 3D printed adapter was used to ensure that the plungers made contact only with the load cell during operation. The sensor is once again connected to a DC power supply and its output is measured using a Keithley[®] 2450 sourcemeter operated as a voltmeter.

ACKNOWLEDGMENTS

General: We are thankful to Sreedath Panat and Caroline McCue for valuable discussions related to this work. **Funding:** We are grateful for support from the Bill and Melina Gates Foundation (Award ID: 026231-00002). **Author Contributions:** V.J. and K.K.V. conceived the project. V.J. carried out the experiments. S.D. carried out fluid characterization. V.J, M.C, S.D and K.K.V. analyzed the data and wrote the paper. K.K.V. supervised the work. **Competing Interests:** V.J, M.C and K.K.V are inventors on a patent application related to this work that has been filed by MIT (US Provisional Application No.: 62/967,239, filed on January 29 2020). The authors declare no other competing interests. **Data and materials availability:** All data needed to evaluate the conclusions in the paper are present in the paper and/or the Supplementary Materials. Additional data related to this paper may be requested from the authors.

References

- [1] *Pharmaceutical Research and Manufacturers of America. Medicines in Development — Biologics (2013 Report). PhRMA [Online], [Http://Www.Phrma.Org/Sites/Default/Files/Pdf/Biologics2013.Pdf](http://www.phrma.org/sites/default/files/pdf/biologics2013.pdf) (2013)., n.d.*
- [2] *Biotech Products in Big Pharma Clinical Pipelines Have Grown Dramatically, Tufts Center For The Study Of Drug Development, 2013.*
- [3] O. H. Brekke, I. Sandlie, *Nat. Rev. Drug Discov.* **2003**, 2, 52.
- [4] S. Awwad, U. Angkawinitwong, S. Awwad, U. Angkawinitwong, *Pharmaceutics* **2018**, 10, 83.
- [5] I. Kimiz-Gebologlu, S. Gulce-Iz, C. Biray-Avci, *Mol. Biol. Rep.* **2018**, 45, 2935.
- [6] L. Hviid, L. Barfod, *Trends Parasitol.* **2008**, 24, 392.
- [7] D. Michaeli, *Semin. Oncol.* **2005**, 32, 82.
- [8] P. Garidel, A. B. Kuhn, L. V. Schäfer, A. R. Karow-Zwick, M. Blech, *Eur. J. Pharm. Biopharm.* **2017**, 119, 353.
- [9] C. Narasimhan, H. Mach, M. Shameem, *Ther. Deliv.* **2012**, 3, 889.
- [10] S. Yadav, S. J. Shire, D. S. Kalonia, *J. Pharm. Sci.* **2010**, 99, 4812.
- [11] J. J. Hung, A. U. Borwankar, B. J. Dear, T. M. Truskett, K. P. Johnston, *J. Memb. Sci.* **2016**, 508, 113.
- [12] V. K. Sharma, T. W. Patapoff, B. Kabakoff, S. Pai, E. Hilario, B. Zhang, C. Li, O. Borisov, R. F. Kelley, I. Chorny, et al., *Proc. Natl. Acad. Sci.* **2014**, 111, 18601.
- [13] D. S. Tomar, L. Li, M. P. Broulidakis, N. G. Luksha, C. T. Burns, S. K. Singh, S. Kumar, *MAbs*

2017, 9, 476.

- [14] A. B. Swanson, I. B. Matev, G. de Groot, *Bull Prosthet Res* **1970**, 10, 145.
- [15] A. Vo, M. Doumit, G. Rockwell, *J. Med. Eng.* **2016**, 2016, DOI 10.1155/2016/5162394.
- [16] V. Burckbuchler, G. Mekhloufi, A. P. Giteau, J. L. Grossiord, S. Huille, F. Agnely, *Eur. J. Pharm. Biopharm.* **2010**, 76, 351.
- [17] L. Arendt-Nielsen, H. Egekvist, P. Bjerring, *Somatosens. Mot. Res.* **2006**, 23, 37.
- [18] S. Mitragotri, P. A. Burke, R. Langer, *Nat. Rev. Drug Discov.* **2014**, 13, 655.
- [19] P. . Hoffman, R. . Abuknesha, N. . Andrews, D. Samuel, J. . Lloyd, *Vaccine* **2001**, 19, 4020.
- [20] H. Suriaa, R. Van Enk, R. Gordon, L. A. Mattano, *Am. J. Infect. Control* **1999**, 27, 444.
- [21] K. Kelly, A. Loskutov, D. Zehrung, K. Puaa, P. LaBarre, N. Muller, W. Guiqiang, H. Ding, D. Hu, W. C. Blackwelder, *Vaccine* **2008**, 26, 1344.
- [22] C. Coffman, L. Charles, P. Brown, D. B. Dandon, L. Liu, S. Shadbar, C. Sudrik, *Particles Comprising a Therapeutic or Diagnostic Agent and Suspensions and Methods of Use Thereof*, **2017**, WIPO PCT: WO2019226969A1.
- [23] O. Qutachi, E. J. Wright, G. Bray, O. A. Hamid, F. R. A. J. Rose, K. M. Shakesheff, D. Delcassian, **2018**, DOI 10.1016/j.ijpharm.2018.05.025.
- [24] M. A. Whitaker, P. Langston, A. Naylor, B. J. Azzopardi, S. M. Howdle, **n.d.**, DOI 10.1007/s10856-011-4359-7.
- [25] J. J. Stickel, R. L. Powell, *Annu. Rev. Fluid Mech.* **2005**, 37, 129.
- [26] R. V. A. Oliemans, G. Ooms, in *Multiph. Sci. Technol.*, Springer Berlin Heidelberg, Berlin,

This article is protected by copyright. All rights reserved.

Heidelberg, **1986**, pp. 427–476.

- [27] D. D. Joseph, R. Bai, K. P. Chen, Y. Y. Renardy, *Annu. Rev. Fluid Mech.* **1997**, *29*, 65.
- [28] S. Ghosh, T. K. Mandal, G. Das, P. K. Das, *Renew. Sustain. Energy Rev.* **2009**, *13*, 1957.
- [29] D. Strazza, B. Grassi, M. Demori, V. Ferrari, P. Poesio, *Chem. Eng. Sci.* **2011**, *66*, 2853.
- [30] J. K. Nunes, S. S. H. Tsai, J. Wan, H. A. Stone, *J. Phys. D. Appl. Phys.* **2013**, *46*, 114002.
- [31] P. Zhu, L. Wang, *Lab Chip* **2017**, *17*, 34.
- [32] T. Cubaud, T. G. Mason, *Phys. Fluids* **2008**, *20*, 053302.
- [33] Z. Zhang, Y. Liu, *Curr. Opin. Chem. Eng.* **2017**, *16*, 48.
- [34] S. J. Shire, in *Monoclon. Antibodies*, Elsevier, **2015**, pp. 131–138.
- [35] D. V. Boger, *Annu. Rev. Fluid Mech.* **1987**, *19*, 157.
- [36] C. Berteau, O. Filipe-Santos, T. Wang, H. E. Rojas, C. Granger, F. Schwarzenbach, *Med. Devices (Auckl)*. **2015**, *8*, 473.
- [37] M. Bentwich, *J. Basic Eng.* **1964**, *86*, 669.
- [38] M. Bentwich, D. A. I. Kelly, N. Epstein, *J. Basic Eng.* **1970**, *92*, 32.
- [39] K. Yoshino, K. Nakamura, A. Yamashita, Y. Abe, K. Iwasaki, Y. Kanazawa, K. Funatsu, T. Yoshimoto, S. Suzuki, *J. Pharm. Sci.* **2014**, *103*, 1520.
- [40] H. Foroughi, M. Kawaji, *Int. J. Multiph. Flow* **2011**, *37*, 1147.
- [41] A. Salim, M. Fourar, J. Pironon, J. Sausse, *Can. J. Chem. Eng.* **2008**, *86*, 978.
- [42] S. Ascarateil, A. Puget, M.-E. Koziol, *J. Immunother. Cancer* **2015**, *3*, P428.

- [43] E. Van Doorn, H. Liu, A. Huckriede, E. Hak, *Hum. Vaccines Immunother.* **2016**, *12*, 159.
- [44] J. Aucouturier, L. Dupuis, S. Deville, S. Ascarateil, V. Ganne, *Expert Rev. Vaccines* **2002**, *1*, 111.
- [45] G. Kretzmer, K. Schöberl, *Appl. Microbiol. Biotechnol.* **1991**, *34*, 613.
- [46] A. W. Tilles, H. Baskaran, P. Roy, M. L. Yarmush, M. Toner, *Biotechnol. Bioeng.* **2001**, *73*, 379.
- [47] M. A. Skylar-Scott, S. G. M. Uzel, L. L. Nam, J. H. Ahrens, R. L. Truby, S. Damaraju, J. A. Lewis, *Sci. Adv.* **2019**, *5*, DOI 10.1126/sciadv.aaw2459.
- [48] B. A. Aguado, W. Mulyasmita, J. Su, K. J. Lampe, S. C. Heilshorn, *Tissue Eng. - Part A* **2012**, *18*, 806.
- [49] G. D'Errico, O. Ortona, F. Capuano, V. Vitagliano, *J. Chem. Eng. Data* **2004**, *49*, 1665.

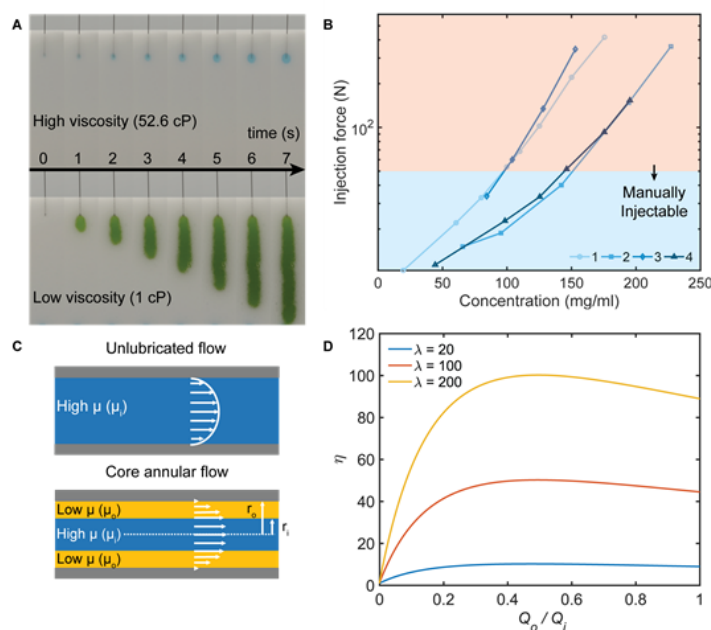


Figure 1: (a) Demonstrates the difficulty in the manual injection of a high viscosity solution (52cP glycerol/water, blue) compared to low viscosity solution (1cP water, green) through a 27G needle. The time-lapse image was taken over 7 seconds of manual injection into an absorbent sponge. The operator applied the maximum pinching force possible (approximately 50N) (b) The force required to manually inject four (labeled 1-4) highly concentrated monoclonal antibody solutions of the IgG1 isotype reported in literature exceeds the maximum force that is applicable in a pinching motion (50N). ^[10-16] (Forces calculated for a flow rate of 4ml/min) (c) Schematic cross-sections of unlubricated flow and core annular flow through a needle. (d) The pressure reduction coefficient (η) scales with the viscosity ratio (λ) between the formulation and the lubricant, demonstrating the promise of core annular flow as a methodology to make any formulation injectable.

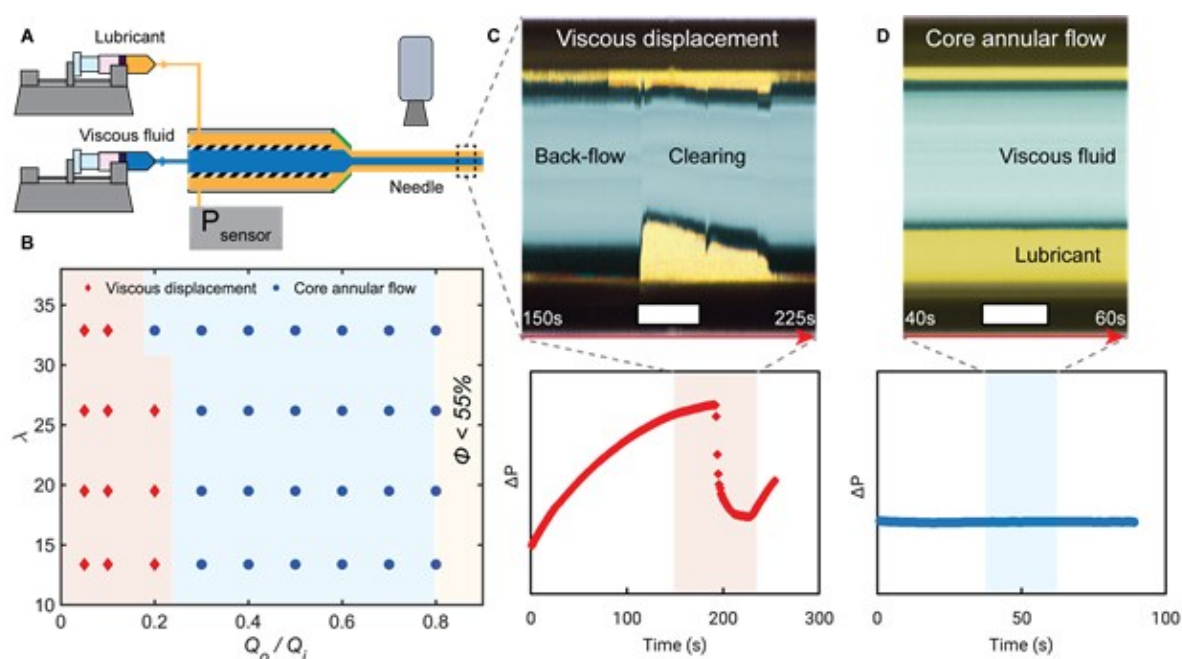


Figure 2: (a) Experimental setup used to study flow regimes and the lubrication effect of core annular flows. (b) Flow regimes observed in the needle for the chosen flow rates. Volume fractions below 55% were not experimentally explored as it is not of interest from a drug injectability perspective. (c) False-colored temporal diagram of a cross-section of the needle (needle inner diameter = 304.8 μm) combined with a pressure versus time plot, highlighting the viscous displacement regime. This regime involves cyclic switching between a primary state where the viscous fluid fills the entire cross-section of the needle to a second state where the two fluids flow as an intermittent core annular flow. This results in a high and unstable pressure drop in the needle. (d) The core annular flow regime, on the other hand, is stable over time and results in a much lower steady-state pressure drop, which is essential to enhance injectability. The scale bars are 100 μm wide.

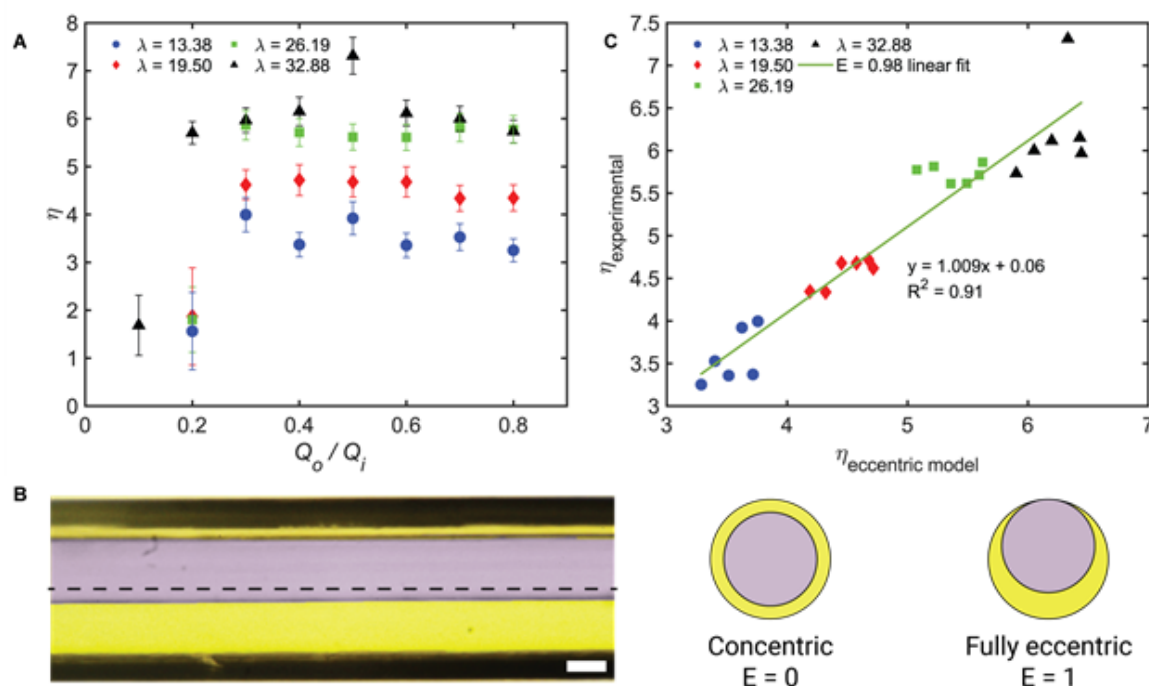


Figure 3: (a) Experimental results show that the pressure reduction coefficient follows a similar trend to concentric core annular flow theory. The pressure reduction coefficient (η) is plotted as a function of the ratio between the lubricant (Q_o) and viscous fluid (Q_i) flow rates for different viscosity ratios (λ). (b) The maximum pressure reduction coefficient is still lower than expected, compared to concentric flow theory for all the viscosity ratios and this reduced performance is attributed to the eccentricity of the viscous fluid due to the density difference between the two fluids. A false-colored digital photograph of the needle demonstrates this eccentricity (needle inner diameter = 304.8 μm , scale bar is 100 μm wide). (c) Illustrates that the performance limit is indeed well described by laminar eccentric core annular flow theory ($E = 0.98$ used for the eccentric model).

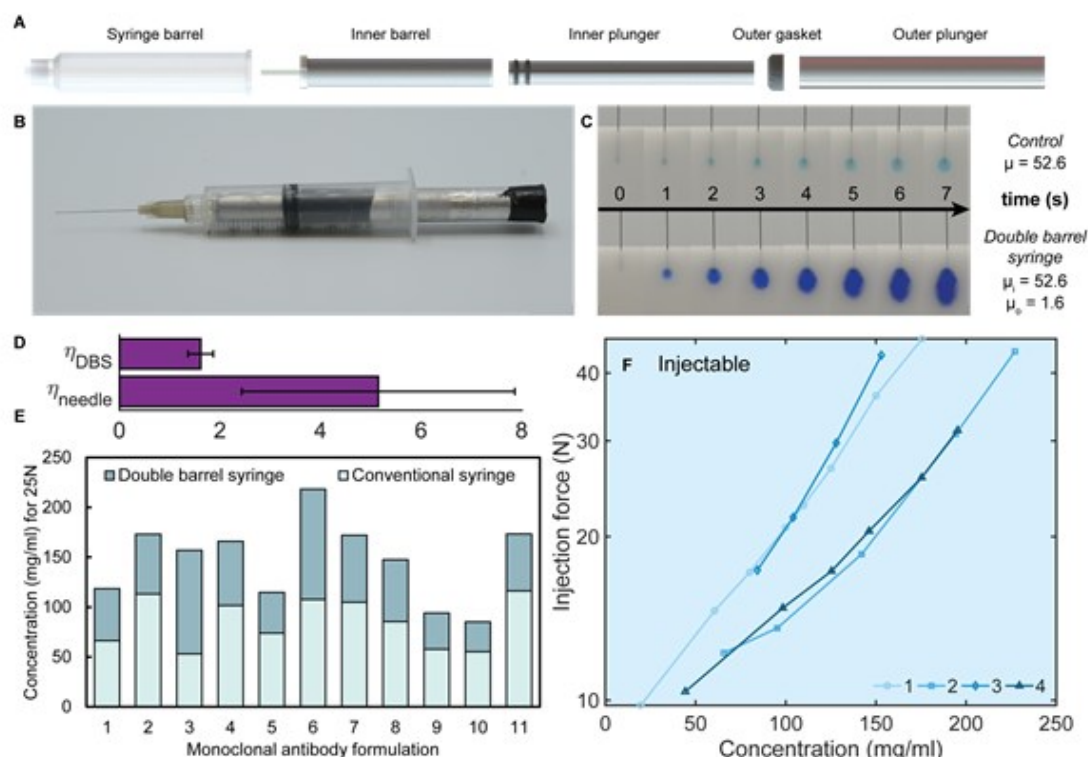


Figure 4: (a) Exploded view of the proof-of-concept double barreled syringe. (b) Photograph of the double barreled syringe (c) Time-lapse images comparing the injectability of a high viscosity formulation through a commercial syringe (light blue) and the double barreled syringe (dark blue). (d) Force reduction coefficient of the overall double barreled syringe (η_{DBS}) and the needle (η_{needle}) alone. (e) Demonstrates the increases in concentrations that are possible for eleven high concentration monoclonal antibody solutions of the IgG1 isotype reported in literature for a nominal injection force of 25N by using the double barreled syringe ^[10-13]. (f) Using $E = 0.98$, the predicted injection forces for four formulations from literature are calculated as a function of monoclonal antibody concentration. Compared to their corresponding values in commercial medical syringes (figure 1b), we show that the regime of injectable concentrations can be expanded significantly using core annular flows. ^[10-16]

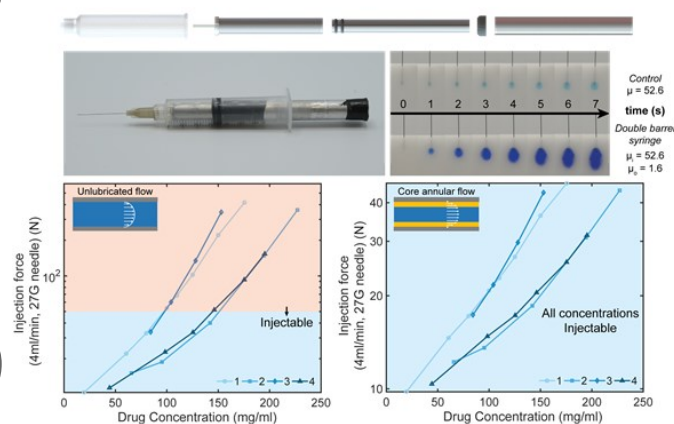
Table of Contents Entry:

A new methodology to inject highly viscous drug formulations subcutaneously using core annular flows is developed. In such a flow, the viscous formulation is lubricated axially by a less viscous fluid. A 7x reduction in injection force is achieved for the highest viscosity ratio tested. As a practical embodiment, a proof-of-concept double barrel syringe is fabricated, expanding the range of injectable viscosities considerably compared to conventional syringes without a significant increase in price.

Keyword: Drug Delivery Device

Authors: Vishnu Jayaprakash, Maxime Costalonga, Somayajulu Dhulipala and Kripa K. Varanasi*

Enhancing the injectability of high concentration drug formulations using core annular flows



This article is protected by copyright. All rights reserved.